Finite amplitude method for the solution of the random-phase approximation

Takashi Nakatsukasa,[1,2,*] Tsunenori Inakura,[2] and Kazuhiro Yabana[1,2]
[1]*Center for Computational Sciences, University of Tsukuba, Tsukuba 305-8571, Japan*
[2]*Institute of Physics, University of Tsukuba, Tsukuba 305-8571, Japan*
(Received 1 April 2007; revised manuscript received 10 July 2007; published 27 August 2007)

We propose a practical method for solving the random-phase approximation (RPA) in the self-consistent Hartree-Fock (HF) and density-functional theory. The method is based on numerical evaluation of the residual interactions utilizing the finite amplitude of single-particle wave functions. The method only requires calculations of the single-particle Hamiltonian constructed with independent bra and ket states. Using the present method, the RPA calculation becomes possible with a little extension of a numerical code of the static HF calculation. We demonstrate the usefulness and accuracy of the present method by performing test calculations for isoscalar responses in deformed ^{20}Ne.

DOI: 10.1103/PhysRevC.76.024318 PACS number(s): 21.60.Jz, 21.10.Pc, 27.30.+t

I. INTRODUCTION

The mean-field theory with a density-dependent effective interaction has been an essential tool in understanding nuclei. Thanks to high performance computing, it is now becoming the most promising tool for the quantitative description of nuclear structure in medium-to-heavy nuclei [1,2]. Nuclear self-consistent mean-field theories are analogous to the density-functional theory in condensed matter. A current major goal is to construct a universal energy-density functional that can describe ground and excited states in nuclei and nuclear matter. This functional is also urgently needed for predicting and interpreting new data from the next generation of radioactive beam facilities.

To describe dynamical properties in nuclear response to external fields, the random-phase approximation (RPA) is a leading theory applicable to both low-lying states and giant resonances [3]. The RPA is a microscopic theory which can be obtained by linearizing the time-dependent Hartree-Fock (TDHF) equation, or equivalently, the time-dependent Kohn-Sham equation in the density-functional theory. The linearization produces a self-consistent residual interaction, $v = \delta^2 E[\rho]/\delta\rho^2$, where E and ρ are the energy-density functional and the one-body density, respectively (Sec. II). The standard solution of the RPA is based on the matrix formulation of the RPA equation, which involves a large number of particle-hole matrix elements of the residual interaction, $v_{\mathrm{ph}',\mathrm{hp}'}$ and $v_{\mathrm{pp}',\mathrm{hh}'}$. Since the realistic nuclear energy functional is rather complicated, it is very tedious and difficult to calculate all the necessary matrix elements. It is, therefore, the purpose of the present paper to present an alternative method of solving the RPA equations in which we deal with only the single-particle Hamiltonian, $h[\rho]$.

Although there are numerous works on the HF-plus-RPA calculations, because of the complexity of the residual interactions, it has been common in practice to neglect some parts of the residual interactions. The RPA calculations with full self-consistency are becoming a current trend in nuclear structure studies; however, they are essentially only for spherical nuclei at present [4–7]. The applications to deformed nuclei are very few, but they have been done for the Skyrme energy functional using the three-dimensional mesh-space representation [8–11]. See Sec. I in Ref. [4] for a current status of these studies.

The basic idea of the present method is analogous to linear-response calculations in a time-dependent manner (real-time method) [8,11,12]. In the real-time method, the time evolution of a TDHF state involves only the action of the HF Hamiltonian, $h[\rho(t)]$, onto single-particle orbitals, $|\psi_i(t)\rangle$ $(i = 1, \ldots, A)$. Although the real-time method is very efficient for obtaining nuclear response in a wide energy range, its numerical instability caused by zero modes was a problem for the linear-response calculations [11]. Zero-energy modes related to symmetry breaking in the HF state are easily excited, which often prevents the calculation of the time evolution for a long period. Therefore, it is desirable to develop a corresponding method in the frequency (energy) representation.

This paper is organized as follows. A new approach to the solution of the linear-response equation, the "finite amplitude method," is presented in Sec. II. The method is named after the "finite difference method" for numerical differentiation. In Sec. II B, we propose a similar numerical method for the functional derivative $\partial h[\rho]/\partial\rho$ to calculate the RPA residual interaction. In Sec. III, using the Bonche-Koonin-Negele (BKN) interaction [13], we check the accuracy of solutions obtained with the present method. We also investigate the zero-energy components in calculated strength functions. Then, the conclusion is summarized in Sec. IV.

II. LINEAR-RESPONSE THEORY

A. TDHF and linear-response equation

The RPA equation is known to be equivalent to the TDHF equation in the small-amplitude limit [3,14]. First, we recapitulate how the standard RPA equation is derived from the small-amplitude TDHF equation, which will help explain the basic idea of our method in Sec. II B.

The HF and TDHF equations can be written in simple form by using the one-body density matrix ρ [3]. The HF

[*]Present address: RIKEN, Wako 351-0198, Japan.

Hamiltonian, $h[\rho] = \delta E[\rho]/\delta\rho$, is a functional of ρ which satisfies the condition $\rho^2 = \rho$. This condition means that the state is expressed by a single Slater determinant. The stationary condition is

$$[h[\rho], \rho] = 0, \tag{1}$$

which defines the HF ground state density $\rho = \rho_0$. Hereafter, the static HF Hamiltonian is simply denoted as $h_0 = h[\rho_0]$, and $\hbar = 1$ is used. When a time-dependent external perturbation is present, the time evolution of the density, $\rho(t)$, follows the TDHF equation

$$i\frac{d}{dt}\rho(t) = [h[\rho(t)] + V_{\rm ext}(t), \rho(t)]. \tag{2}$$

Using this $\rho(t)$, the expectation value of a one-body operator F is obtained as $\langle F\rangle = {\rm tr}\{F\rho(t)\}$. Provided that the perturbation is weak, we may linearize Eq. (2) with respect to $V_{\rm ext}(t)$ and $\delta\rho(t)$ defined by

$$\rho(t) = \rho_0 + \delta\rho(t). \tag{3}$$

This leads to a time-dependent linear-response equation with an external field, that is,

$$i\frac{d}{dt}\delta\rho(t) = [h_0, \delta\rho(t)] + [V_{\rm ext}(t) + \delta h(t), \rho_0], \tag{4}$$

where $\delta h(t)$ is a residual field induced by density fluctuations,

$$\delta h(t) \equiv \frac{\delta h}{\delta\rho}\cdot\delta\rho(t) = \sum_{\mu\nu}\left.\frac{\partial h}{\partial\rho_{\mu\nu}}\right|_{\rho=\rho_0}\delta\rho_{\mu\nu}(t). \tag{5}$$

It should be noted that $\delta h(t)$ has a linear dependence on $\delta\rho(t)$. As we will see in Eq. (15), if we adopt the natural basis diagonalizing h_0, the summation can be restricted to the particle-hole ($\mu > A, \nu \leqslant A$) and hole-particle ($\mu \leqslant A, \nu > A$) components. Now, we decompose the time-dependent $\delta\rho(t)$ into those with fixed frequencies:

$$\delta\rho(t) = \sum_\omega\{\eta\delta\rho(\omega)e^{-i\omega t} + \eta^*\delta\rho^\dagger(\omega)e^{i\omega t}\}. \tag{6}$$

The external and induced fields are also expressed in the same way:

$$\delta h(t) = \sum_\omega\{\eta\delta h(\omega)e^{-i\omega t} + \eta^*\delta h^\dagger(\omega)e^{i\omega t}\}, \tag{7}$$

$$V_{\rm ext}(t) = \sum_\omega\{\eta V_{\rm ext}(\omega)e^{-i\omega t} + \eta^* V_{\rm ext}^\dagger(\omega)e^{i\omega t}\}. \tag{8}$$

Here, we have introduced a small dimensionless parameter η. $\delta h(\omega)$ may be written as $\delta h(\omega) = \delta h/\delta\rho\cdot\delta\rho(\omega)$. Note that the transition density, the external field, and the induced field in the ω representation, $\delta\rho(\omega)$, $V_{\rm ext}(\omega)$, and $\delta h(\omega)$, are not necessarily Hermitian. Substituting these into the linearized TDHF equation (4), we obtain the linear-response equation in the frequency representation,

$$\omega\,\delta\rho(\omega) = [h_0, \delta\rho(\omega)] + [V_{\rm ext}(\omega) + \delta h(\omega), \rho_0]. \tag{9}$$

This is the equation we want to solve in this paper.

When the frequency ω is equal to an RPA eigenfrequency ω_n, there is a nonzero solution, $\delta\rho_n$, of Eq. (9) with $V_{\rm ext} = 0$. These are called normal modes and are orthogonal to each other. The orthonormalization is given by

$${\rm tr}\{[\delta\rho_n^\dagger, \delta\rho_{n'}]\rho_0\} = \langle\Phi_0|[\delta\rho_n^\dagger, \delta\rho_{n'}]|\Phi_0\rangle = \delta_{nn'}, \tag{10}$$

where $|\Phi_0\rangle$ indicates the HF ground state. Later, we will introduce forward and backward amplitudes in Eq. (19). It is easy to see from Eqs. (17) and (19) that Eq. (10) is equivalent to a more familiar expression [3],

$$\sum_{mi}\left(X_{mi}^{(n)*}X_{mi}^{(n')} - Y_{mi}^{(n)*}Y_{mi}^{(n')}\right) = \delta_{nn'}. \tag{11}$$

Equation (10) also tells us that to normalize the transition density $\delta\rho_n$, it must be non-Hermitian. When $\omega = \omega_n$, the nucleus is truly excited by $V_{\rm ext}(\omega)$, and we cannot determine the magnitude of $\delta\rho(\omega_n)$ because $\delta\rho(t)$ increases in time. If $\delta\rho(\omega_n)$ is a solution of Eq. (9), then $\delta\rho(\omega_n) + c\delta\rho_n$ with an arbitrary constant c is also a solution.

So far, the linear-response equation has been expressed in terms of the one-body density operators. The density-matrix formulation is simple and easy to manipulate; in practical calculations, however, it is convenient to introduce single-particle (Kohn-Sham) orbitals. For systems with A particles, the TDHF describes the one-body density using A single-particle orbitals, $|\psi_i(t)\rangle$, as

$$\rho(t) = \sum_{i=1}^{A}|\psi_i(t)\rangle\langle\psi_i(t)|, \quad \rho_0 = \sum_{i=1}^{A}|\phi_i\rangle\langle\phi_i|. \tag{12}$$

It is an advantage of the TDHF that the time evolution is described only by occupied orbitals, i.e., $\{|\psi_i\rangle\}$ with $i = 1, \ldots, A$. The static orbitals are normally chosen as eigenstates of the HF Hamiltonian,

$$h_0|\phi_\mu\rangle = \epsilon_\mu|\phi_\mu\rangle, \tag{13}$$

which can be divided into two categories: occupied (hole) orbitals, $\{\phi_i\}$ ($i = 1, \ldots, A$), for which we use indexes $i, j, \ldots$, and unoccupied (particle) orbitals, $\{\phi_m\}$ ($m = A+1, \ldots$), for which we use indexes $m, n, \ldots$. In the linear approximation, we have

$$\delta\rho(t) = \sum_i\{|\phi_i\rangle\langle\delta\psi_i(t)| + |\delta\psi_i(t)\rangle\langle\phi_i|\}, \tag{14}$$

where $|\psi_i(t)\rangle = (|\phi_i\rangle + |\delta\psi_i(t)\rangle)e^{-i\epsilon_i t}$, and it is linearized with respect to $|\delta\psi_i(t)\rangle$. The condition $\rho(t)^2 = \rho(t)$ leads to

$$\delta\rho_{ij} = \delta\rho_{mn} = 0, \quad i,\ j \leqslant A, \quad m,\ n > A, \tag{15}$$

$$\langle\phi_j|\delta\psi_i\rangle + \langle\delta\psi_j|\phi_i\rangle = 0. \tag{16}$$

The second equation is nothing but the orthonormalization condition for single-particle orbitals, $\{|\psi_i(t)\rangle\}$ ($i = 1, \ldots, A$).

Transforming $\delta\rho(t)$ into $\delta\rho(\omega)$ in Eq. (6), we must make ket and bra states independent, because $\delta\rho(\omega)$ is not Hermitian. This is related to the fact that the RPA equation is described by forward and backward amplitudes, $X(\omega)$ and $Y(\omega)$.

$$\delta\rho(\omega) = \sum_i\{|X_i(\omega)\rangle\langle\phi_i| + |\phi_i\rangle\langle Y_i(\omega)|\}. \tag{17}$$

This is equivalent to the Fourier decomposition of the time-dependent single-particle orbitals [15],

$$|\delta\psi_i(t)\rangle = \sum_{\omega}\{\eta|X_i(\omega)\rangle e^{-i\omega t} + \eta^*|Y_i(\omega)\rangle e^{i\omega t}\}. \tag{18}$$

Since only the particle-hole matrix elements of $\delta\rho(\omega)$ are nonzero, seen in Eq. (15), we can assume that the amplitudes $|X_i(\omega)\rangle$ and $|Y_i(\omega)\rangle$ can be expanded in the particle orbitals only, that is,

$$|X_i(\omega)\rangle = \sum_{m>A}|\phi_m\rangle X_{mi}(\omega), \quad |Y_i(\omega)\rangle = \sum_{m>A}|\phi_m\rangle Y^*_{mi}(\omega). \tag{19}$$

If we take particle-hole and hole-particle matrix elements of Eq. (9) with the help of Eqs. (17) and (19), we can derive the well-known RPA equation in the matrix form [3]

$$\left\{\begin{pmatrix} A & B \\ B^* & A^* \end{pmatrix} - \omega\begin{pmatrix} 1 & 0 \\ 0 & -1 \end{pmatrix}\right\}\begin{pmatrix} X_{nj}(\omega) \\ Y_{nj}(\omega) \end{pmatrix} = -\begin{pmatrix} f(\omega) \\ g(\omega) \end{pmatrix}. \tag{20}$$

Here, matrices A and B and vectors f and g are defined by

$$A_{mi,nj} \equiv (\epsilon_m - \epsilon_i)\delta_{mn}\delta_{ij} + \langle\phi_m|\left.\frac{\partial h}{\partial\rho_{nj}}\right|_{\rho=\rho_0}|\phi_i\rangle, \tag{21}$$

$$B_{mi,nj} \equiv \langle\phi_m|\left.\frac{\partial h}{\partial\rho_{jn}}\right|_{\rho=\rho_0}|\phi_i\rangle, \tag{22}$$

$$f_{mi}(\omega) \equiv \langle\phi_m|V_{\rm ext}(\omega)|\phi_i\rangle, \quad g_{mi}(\omega) \equiv \langle\phi_i|V_{\rm ext}(\omega)|\phi_m\rangle. \tag{23}$$

This is a standard matrix formulation of the RPA equation. In practical applications, the most tedious part is the calculation of matrix elements of the residual interactions in $A_{mi,nj}$ and $B_{mi,nj}$. In Ref. [16], a numerical method to solve the RPA equation in the coordinate space is proposed, and similar approaches are used in realistic applications using the Skyrme interaction [9,10]. In those works, one does not need to calculate the particle orbitals; however, the residual interaction must be evaluated in the coordinate-space representation. In Sec. II B, we propose an even simpler alternative approach to a solution of the linear-response equation (9). The method does not require explicit evaluation of the residual interaction, $\delta h/\delta\rho$.

B. Finite amplitude method

Multiplying both sides of Eq. (9) with a ket of hole states $|\phi_i\rangle$, we have

$$\omega|X_i(\omega)\rangle = (h_0 - \epsilon_i)|X_i(\omega)\rangle + \hat{Q}\{V_{\rm ext}(\omega) + \delta h(\omega)\}|\phi_i\rangle, \tag{24}$$

where $\hat{Q}$ is a projection operator onto the particle space, $\hat{Q} = 1 - \sum_j|\phi_j\rangle\langle\phi_j|$. Another equation can be derived by multiplying a bra state $\langle\phi_i|$ with Eq. (9):

$$\omega\langle Y_i(\omega)| = -\langle Y_i(\omega)|(h_0 - \epsilon_i) - \langle\phi_i|\{V_{\rm ext}(\omega) + \delta h(\omega)\}\hat{Q}. \tag{25}$$

These are formally equivalent to the RPA equation in the matrix form of Eq. (20).

The essential idea of our new numerical approach is as follow: Eqs. (24) and (25) require operations of the HF Hamiltonian in the ground state h_0 and the induced fields $\delta h(\omega)$ and $\delta h^\dagger(\omega)$. Since h_0 is obtained by the static HF calculation, a new ingredient for the RPA calculation is the latter two. The conventional approach is to expand $\delta h(\omega)$ in the linear order as Eq. (5), then to solve the RPA equation in a matrix form. In this paper, instead of performing the explicit expansion, we resort to the numerical linearization. Now, let us explain how to achieve it.

The time-dependent self-consistent Hamiltonian, $h(t) = h[\rho(t)]$, is a functional of one-body density that is represented by occupied A single-particle orbitals. We may regard it as a functional of A single-particle orbitals, $h[\psi(t)]$. In the linear approximation, the induced field can be written as

$$\delta h(t) = h[\rho_0 + \delta\rho(t)] - h_0 = h[\phi + \delta\psi(t)] - h_0. \tag{26}$$

In the frequency representation, the story becomes slightly more complicated, because $\delta h(\omega)$ and $\delta h^\dagger(\omega)$ are no longer Hermitian. In this case, we should regard the HF Hamiltonian as a functional of $2A$ single-particle states (independent bra and ket), $\langle\psi'_i|$ and $|\psi_i\rangle$, $i = 1, \ldots, A$. We denote it as $h\big[\langle\psi'|, |\psi\rangle\big]$. Using Eq. (17), we may write the non-Hermitian density as

$$\rho_0 + \eta\delta\rho(\omega) = \sum_i\{|\phi_i\rangle\langle\phi_i| + \eta|X_i(\omega)\rangle\langle\phi_i| + \eta|\phi_i\rangle\langle Y_i(\omega)|\} \tag{27}$$

$$= \sum_i\{|\phi_i\rangle + \eta|X_i(\omega)\rangle\}\{\langle\phi_i| + \eta\langle Y_i(\omega)|\}. \tag{28}$$

In the last equation, we assume the linear approximation with respect to η. The fact that $\delta h(\omega)$ is proportional to $\delta\rho(\omega)$ and $\delta h^\dagger(\omega)$ is proportional to $\delta\rho^\dagger(\omega)$ leads to

$$h_0 + \eta\,\delta h(\omega) = h[\rho_0 + \eta\delta\rho(\omega)] = h[\langle\phi| + \eta\langle Y(\omega)|, |\phi\rangle + \eta|X(\omega)\rangle], \tag{29}$$

$$h_0 + \eta\,\delta h^\dagger(\omega) = h[\rho_0 + \eta\delta\rho^\dagger(\omega)] = h[\langle\phi| + \eta\langle X(\omega)|, |\phi\rangle + \eta|Y(\omega)\rangle]. \tag{30}$$

In other words, the induced fields may be calculated using the finite difference with respect to η, that is,

$$\delta h(\omega) = \frac{1}{\eta}(h[\langle\psi'|, |\psi\rangle] - h[\langle\phi|, |\phi\rangle]), \tag{31}$$

where $\langle\psi'_i| = \langle\phi_i| + \eta\langle Y_i(\omega)|$ and $|\psi_i\rangle = |\phi_i\rangle + \eta|X_i(\omega)\rangle$. Its Hermitian conjugate, $\delta h^\dagger(\omega)$, may be expressed as the same equation (31), but with $\langle\psi'_i| = \langle\phi_i| + \eta\langle X_i(\omega)|$ and $|\psi_i\rangle = |\phi_i\rangle + \eta|Y_i(\omega)\rangle$.

Using these numerical differentiation, the right-hand side of the RPA equations (24) and (25) can be easily calculated by action of the HF Hamiltonian $h\big[\langle\psi'|, |\psi\rangle\big]$ on the single-particle orbitals $|\phi_i\rangle$. At first, Eqs. (24) and (25) do not look like linear equations. However, since $\delta h(\omega)$ linearly depends on $|X_i(\omega)\rangle$ and $\langle Y_i(\omega)|$, they are inhomogeneous linear equations with respect to $|X_i(\omega)\rangle$ and $\langle Y_i(\omega)|$. Therefore, we can employ a well-established iterative method for their solution. If the linear equation is described by a Hermitian matrix, the conjugate gradient method (CGM) is one of the most powerful methods.

However, in general, we may take the frequency ω complex, and then the RPA matrix becomes non-Hermitian. For this, we should use another kind of iterative solver, for instance, the biconjugate gradient method (Bi-CGM). A typical numerical procedure is as follows: (i) Fix the frequency ω which can be complex and assume initial vectors ($n = 0$) as $|X_i^{(n)}(\omega)\rangle$ and $\langle Y_i^{(n)}(\omega)|$. (ii) Update the vectors $|X_i^{(n+1)}(\omega)\rangle$ and $\langle Y_i^{(n+1)}(\omega)|$ using the algorithm of an iterative method, such as CGM or Bi-CGM. (iii) Calculate the residual of Eqs. (24) and (25). If its magnitude is smaller than a given accuracy, stop the iteration. Otherwise, go back to step (ii).

The most advantageous feature of the present approach is that it only requires operations of the HF Hamiltonian $h\big[\langle\psi'|, |\psi\rangle\big]$. These are usually included in computational programs of the static HF calculations. The only extra effort necessary is to estimate the HF Hamiltonian with different bra and ket single-particle states, $\langle\psi_i'|$ and $|\psi_i\rangle$. Therefore, a minor modification of the static HF computer code will provide a numerical solution of the RPA equations. Hereafter, we call this numerical approach the "finite amplitude method." Apparently, the present method is also applicable to the RPA eigenvalue problems [9,16] with a trivial modification.

C. Transition strength in the linear response

In this subsection, we explain how to calculate transition strength using the solutions of Eqs. (24) and (25). Assuming that the system is at its ground state $|\Phi_0\rangle$ with energy $E_0 = 0$ at $t = -\infty$, and that the external field $V_{\rm ext}(t)$ is adiabatically switched on [$\omega \to \omega \pm i\epsilon$ in Eq. (8)], the state at time t will be

$$|\Psi(t)\rangle = |\Phi_0\rangle - i\sum_n e^{-iE_nt}\int_{-\infty}^{t} dt' e^{iE_nt'}|\Phi_n\rangle\langle\Phi_n|V_{\rm ext}(t')|\Phi_0\rangle \tag{32}$$

in the first-order approximation with respect to $V_{\rm ext}$. Here, $|\Phi_n\rangle$ and E_n are the nth excited state and its excitation energy, respectively. If the external field has a fixed frequency $\omega > 0$, and $V_{\rm ext}(t) = \eta F e^{-i\omega t} + \eta^* F^\dagger e^{i\omega t}$, then this is written as

$$|\Psi(t)\rangle = |\Phi_0\rangle - i\sum_n |\Phi_n\rangle \times\left(\frac{\eta\langle\Phi_n|F|\Phi_0\rangle}{\omega - E_n + i\epsilon}e^{-i\omega t} - \frac{\eta^*\langle\Phi_n|F^\dagger|\Phi_0\rangle}{\omega + E_n - i\epsilon}e^{i\omega t}\right), \tag{33}$$

where F is an arbitrary one-body operator. Then, the expectation value of $F^\dagger$ at time t is

$$\langle\Psi(t)|F^\dagger|\Psi(t)\rangle \equiv \langle\Phi_0|F^\dagger|\Phi_0\rangle + \eta S(F;\omega)e^{-i\omega t} + \cdots, \tag{34}$$

$$S(F;\omega) = \sum_n\left(\frac{|\langle\Phi_n|F|\Phi_0\rangle|^2}{\omega - E_n + i\epsilon} - \frac{|\langle\Phi_n|F^\dagger|\Phi_0\rangle|^2}{\omega + E_n - i\epsilon}\right). \tag{35}$$

Taking the limit of $\epsilon \to 0$, we have the transition strength

$$\frac{dB(\omega;F)}{d\omega} \equiv \sum_n |\langle\Phi_n|F|\Phi_0\rangle|^2\delta(\omega - E_n) = -\frac{1}{\pi}{\rm Im}S(F;\omega). \tag{36}$$

Comparing Eq. (34) with the expectation value in the TDHF state,

$${\rm tr}\{F^\dagger\rho(t)\} = {\rm tr}\{F^\dagger\rho_0\} + {\rm tr}\{F^\dagger\delta\rho(\omega)\}e^{-i\omega t} + \cdots. \tag{37}$$

$S(F;\omega)$ in the RPA is written as

$$S_{\rm RPA}(F;\omega) = {\rm tr}\{F^\dagger\delta\rho(\omega)\} = i\,{\rm tr}\{[\delta\rho_F^\dagger, \delta\rho(\omega)]\} \tag{38}$$

$$= \sum_i(\langle\phi_i|F^\dagger|X_i(\omega)\rangle + \langle Y_i(\omega)|F^\dagger|\phi_i\rangle). \tag{39}$$

Here, $\delta\rho_F$ is defined by $\delta\rho_F \equiv i[F, \rho_0]$.

D. Separation of Nambu-Goldstone modes

The RPA theory is known to have the property that the zero-energy modes are exactly decoupled from the physical (intrinsic) modes of excitation [3,14]. Since the zero modes are associated with symmetry breaking in the HF ground state, they are also called Nambu-Goldstone (NG) modes. When the Hamiltonian commutes with a Hermitian symmetry operator P, $[H, P] = 0$, the transformed ground state density $\tilde\rho_0 = e^{i\alpha P}\rho_0 e^{-i\alpha P}$ also fulfills the HF equation [3]. Expanding Eq. (1) to the first order in α, we have

$$[h_0, \delta\tilde\rho] + [\delta\tilde h, \rho_0] = 0, \tag{40}$$

where

$$\delta\tilde\rho \equiv \tilde\rho_0 - \rho_0 = i\alpha[P, \rho_0], \quad \delta\tilde h \equiv h[\tilde\rho_0] - h_0 = \frac{\delta h}{\delta\rho}\cdot\delta\tilde\rho. \tag{41}$$

This indicates that $\delta\tilde\rho$ is an RPA eigenmode corresponding to $\omega = 0$. There exists another operator R conjugate to P ($[R, P] = i$) [3]. For instance, the translational symmetry is usually broken in the HF ground state of finite nuclei. The total momentum corresponds to the zero-energy eigenmode, and the center-of-mass coordinate generates the boost mode. We denote these transition densities associated with the NG mode as

$$\delta\rho_P \equiv i[P, \rho_0] = \frac{1}{\alpha}\delta\tilde\rho = \sum_i(|\bar P_i\rangle\langle\phi_i| + |\phi_i\rangle\langle\bar P_i|), \tag{42}$$

$$\delta\rho_R \equiv i[R, \rho_0] = \sum_i(|\bar R_i\rangle\langle\phi_i| + |\phi_i\rangle\langle\bar R_i|), \tag{43}$$

where we have defined $|\bar P_i\rangle \equiv iP|\phi_i\rangle$ and $|\bar R_i\rangle \equiv iR|\phi_i\rangle$ [14]. In principle, the NG modes should be automatically orthogonal to other normal modes. However, in practice, we often encounter a mixture of spurious components in physical excitations. For instance, the coordinate space is discretized in mesh to represent wave functions in Sec. III, which violates the exact translational and rotational symmetries. We also use a smoothing parameter Γ to make the frequency complex; then, low-lying excited states are embedded in a large tail of the NG-mode strength [$\delta\rho(\omega) \to \infty$ for $\omega \to 0$]. For these cases, we need a prescription to remove the strength associated with the NG mode.

Let us assume that there is a mixture of NG modes in a calculated transition density, $\delta\rho_{\rm cal}(\omega)$.

$$\delta\rho_{\rm cal}(\omega) = \delta\rho_{\rm phy}(\omega) + \lambda_P\delta\rho_P + \lambda_R\delta\rho_R, \tag{44}$$

where "physical" transition density $\delta\rho_{\rm phy}(\omega)$ is free from the NG modes. Here, we assume there is a single NG mode, for simplicity. It is straightforward to extend the present prescription to the case for more than one NG mode. Since $\delta\rho_{\rm phy}$ should be orthogonal to the NG modes, we have

$$\langle\Phi_0|[\delta\rho_P, \delta\rho_{\rm phy}(\omega)]|\Phi_0\rangle = \langle\Phi_0|[\delta\rho_R, \delta\rho_{\rm phy}(\omega)]|\Phi_0\rangle = 0. \tag{45}$$

Utilizing the canonicity condition $[R, P] = i$, the orthogonality condition in Eq. (45) determines the coefficients $\lambda_{P(R)}$ as

$$\lambda_P = -i\sum_i(\langle\bar{R}_i|X_i(\omega)\rangle - \langle Y_i(\omega)|\bar{R}_i\rangle), \tag{46}$$

$$\lambda_R = i\sum_i(\langle\bar{P}_i|X_i(\omega)\rangle - \langle Y_i(\omega)|\bar{P}_i\rangle). \tag{47}$$

Substituting these into Eq. (44), we may extract $\delta\rho_{\rm phy}(\omega)$ from the "contaminated" transition density $\delta\rho_{\rm cal}(\omega)$. We will demonstrate in the next section that this prescription nicely removes spurious peaks without affecting other physical modes.

III. NUMERICAL APPLICATIONS

A. Coordinate-space representation

For zero-range effective interactions such as Skyrme interactions, the HF Hamiltonian $h(\mathbf{r}) = h[\rho(\mathbf{r})]$ is a functional of local one-body densities. For these, it is convenient to adopt the coordinate-space representation. In the following, we assume $\mathbf{r}$ involves the spin and isospin indexes, if necessary. The RPA equations (24) and (25) for a complex frequency ω can be written in the $\mathbf{r}$ representation as

$$\begin{aligned}&(h_0(\mathbf{r})-\epsilon_i-\omega)X_i(\mathbf{r},\omega)+\delta h(\mathbf{r},\omega)\phi_i(\mathbf{r})\\&\quad= -V_{\rm ext}(\mathbf{r},\omega)\phi_i(\mathbf{r}),\end{aligned} \tag{48}$$

$$\begin{aligned}&\{(h_0(\mathbf{r}) - \epsilon_i + \omega^*)Y_i(\mathbf{r},\omega) + \delta h^\dagger(\mathbf{r},\omega)\phi_i(\mathbf{r})\}^*\\&\quad= -\{V^\dagger_{\rm ext}(\mathbf{r},\omega)\phi_i(\mathbf{r})\}^*.\end{aligned} \tag{49}$$

Here, for simplicity, we omit the projection operator $\hat{Q}$ on both sides of these equations. In the finite amplitude method, the operation of $\delta h(\mathbf{r},\omega)$ is calculated by

$$\delta h(\mathbf{r},\omega)\phi_i(\mathbf{r}) = \frac{1}{\eta}(h[\psi'^*,\psi](\mathbf{r})\phi_i(\mathbf{r}) - \epsilon_i\phi_i(\mathbf{r})), \tag{50}$$

with $\psi'^*_i(\mathbf{r}) = \phi^*_i(\mathbf{r}) + \eta Y^*_i(\omega,\mathbf{r})$ and $\psi_i(\mathbf{r}) = \phi_i(\mathbf{r}) + \eta X_i(\mathbf{r},\omega)$. Exchanging the forward and backward amplitudes in $\psi_i(\mathbf{r})$ and $\psi'_i(\mathbf{r})$, we may calculate $\delta h^\dagger(\mathbf{r},\omega)\phi_i(\mathbf{r})$ in the same way.

Adopting the fixed-ω local external field

$$V_{\rm ext}(\mathbf{r},\omega') = \delta_{\omega\omega'}F(\mathbf{r}), \tag{51}$$

the transition strength can be obtained from the calculated forward and backward amplitudes, as in Eqs. (36) and (39),

$$\frac{dB(\omega;F)}{d\omega} \equiv \sum_n |\langle n|F|0\rangle|^2\delta(\omega - E_n), \tag{52}$$

$$\begin{aligned}&= -\frac{1}{\pi}{\rm Im}\sum_i\int d\mathbf{r}\{\phi^*_i(\mathbf{r})F^\dagger(\mathbf{r})X_i(\mathbf{r},\omega)\\&\quad + Y^*_i(\mathbf{r},\omega)F^\dagger(\mathbf{r})\phi_i(\mathbf{r})\}.\end{aligned} \tag{53}$$

We apply the present method to the BKN interaction which contains two-body (zero- and finite-range) and three-body interactions. For this schematic interaction, the spin-isospin degeneracy is assumed all the time, and the Coulomb potential acts on all orbitals with a charge $e/2$ [13]. The HF one-body Hamiltonian in the coordinate-space representation is given by

$$\begin{aligned}h[\rho] = &-\frac{1}{2m}\nabla^2 + \frac{3}{4}t_0\rho(\mathbf{r}) + \frac{3}{16}t_3\rho^2(\mathbf{r})\\&+ W_Y[\rho](\mathbf{r}) + W_C[\rho](\mathbf{r}),\end{aligned} \tag{54}$$

where the Yukawa potential W_Y and Coulomb potential W_C consist only of their direct terms. For the finite amplitude approach, it is convenient to rewrite Eq. (54) as

$$\begin{aligned}h[\psi'^*,\psi](\mathbf{r}) = &-\frac{1}{2m}\nabla^2 + \frac{3}{4}t_0\sum_{i=1}^{A/4}4\psi_i(\mathbf{r})\psi'^*_i(\mathbf{r})\\&+\frac{3}{16}t_3\left\{\sum_{i=1}^{A/4}4\psi_i(\mathbf{r})\psi'^*_i(\mathbf{r})\right\}^2\\&+\int d\mathbf{r}'v(\mathbf{r}-\mathbf{r}')\sum_{i=1}^{A/4}4\psi_i(\mathbf{r}')\psi'^*_i(\mathbf{r}'),\end{aligned} \tag{55}$$

where $v(\mathbf{r})$ is a sum of the Yukawa and the Coulomb potentials,

$$v(\mathbf{r}) \equiv V_0 a\frac{e^{-r/a}}{r} + \frac{(e/2)^2}{|\mathbf{r}|}. \tag{56}$$

We adopt the parameter values from Ref. [13].

B. Numerical details

We use the three-dimensional coordinate-space representation for solving the RPA equations. The model space is a sphere of radius of 10 fm, discretized in square mesh of $\Delta x = \Delta y = \Delta z = 0.8$ fm. The number of grid points in the sphere is 8217. The differentiation is approximated by the nine-point formula. The frequency ω is varied from zero to 40 MeV with a spacing of $\Delta\omega = 200$ keV (201 points). A small imaginary part is added to ω: $\omega \to \omega + i\Gamma/2$ with $\Gamma = 500$ keV. In numerical calculations, we use real variables with double precision (8 bytes) and complex variables of 8×2 bytes. In Eq. (50), we choose the parameter η in $\psi_i(\mathbf{r}) = \phi_i(\mathbf{r}) + \eta X_i(\mathbf{r})$ and $\psi'^*_i(\mathbf{r}) = \phi^*_i(\mathbf{r}) + \eta Y^*_i(\mathbf{r})$, as follows:

$$\eta = \frac{10^{-5}}{\max\{N(X), N(Y)\}}, \quad N(\delta\psi) \equiv \frac{1}{A}\sqrt{\sum_i\langle\delta\psi_i|\delta\psi_i\rangle}. \tag{57}$$

To obtain the forward and backward amplitudes at a frequency ω, we adopt the Bi-CGM as an iterative solver for Eqs. (48) and (49), starting from the initial values of $X_i(\mathbf{r}) = Y^*_i(\mathbf{r}) = 0$. We set the convergence condition such that the ratio of the remaining difference to the right-hand side of Eqs. (48) and (49) is less than 10^{-5}. The number of iterations necessary to

reach the convergence depends on the choice of the external field $V_{\rm ext}(\omega)$, the frequency ω, the smoothing parameter Γ, and the residual interactions included in the calculation. The convergence is relatively slow for an external field coupled to the NG modes. A larger number of iterations is required for a larger ω value. Typically, the calculation reaches the convergence in 10–100 iterations for $\omega < 10$ MeV, but it requires more than 500 iterations for $\omega > 30$ MeV. The number also depends on the smoothing parameter Γ. Roughly speaking, a larger number of iterations seems to be required for smaller Γ. If we neglect the residual Coulomb and Yukawa interactions of finite range, the convergence becomes much faster. We solve the differential equations to obtain the Coulomb and Yukawa potentials using the CGM [17]:

$$\nabla^2 V_C = -2\pi e^2 \rho(\mathbf{r}), \quad \left(\nabla^2 - \frac{1}{a^2}\right) V_Y = -4\pi V_0 a \rho(\mathbf{r}). \tag{58}$$

It turns out to be important to solve these equations with high accuracy. We set the convergence condition such that the ratio of the remaining difference to the right-hand side of Eq. (58) is less than 10^{-23}. Since the convergence of the CGM is very fast, this is not a problem.

C. Results

In this section, we show the calculated response for isoscalar (IS) modes of compressional dipole, quadrupole, and octupole for ^{20}Ne. The main purpose of the calculation is to test the capability of the present numerical approach, the finite amplitude method. The ^{20}Ne nucleus has a prolate shape with a quadrupole deformation $\beta \approx 0.4$ in the HF ground state. Identifying the symmetry axis with the z axis, we use external fields with a fixed frequency, $V_{\rm ext}(\mathbf{r}) = Q_{\lambda K}(\mathbf{r})$, where

$$Q_{\lambda K}(\mathbf{r}) = \begin{cases} r^3 Y_{10}(\hat{\mathbf{r}}), \quad r^3 Y_{11}(\hat{\mathbf{r}}), & \text{for IS dipole,} \\ & \lambda = 1, \\ r^2 Y_{20}(\hat{\mathbf{r}}), \quad r^2 Y_{21}(\hat{\mathbf{r}}), \quad r^2 Y_{22}(\hat{\mathbf{r}}), & \\ & \text{for IS quadrupole, } \lambda = 2, \\ r^3 Y_{30}(\hat{\mathbf{r}}), \quad r^3 Y_{31}(\hat{\mathbf{r}}), \quad r^3 Y_{32}(\hat{\mathbf{r}}), \quad r^3 Y_{33}(\hat{\mathbf{r}}), & \\ & \text{for IS octupole, } \lambda = 3. \end{cases} \tag{59}$$

Then, the strength distribution

$$\frac{dB(\omega; Q_{\lambda K})}{d\omega} = \sum_n |\langle n|Q_{\lambda K}|0\rangle|^2 \delta(\omega - E_n) \tag{60}$$

will be calculated according to Eq. (53).

1. Isoscalar quadrupole response: Accuracy of the finite amplitude method

In Fig. 1(a), we show results for the IS quadrupole strength distribution. There is a NG mode in the $K = 1$ sector, corresponding to the nuclear rotation. This is clearly seen in the response of the $K = 1$ mode, having a large peak near $\omega = 0$. The RPA correlation brings the lowest one-particle-one-hole (1p1h) excitation at $E_x = 4.5$ MeV down to zero. The response function for the $K = 1$ mode was not obtained by the small-amplitude TDHF method in Ref. [11],

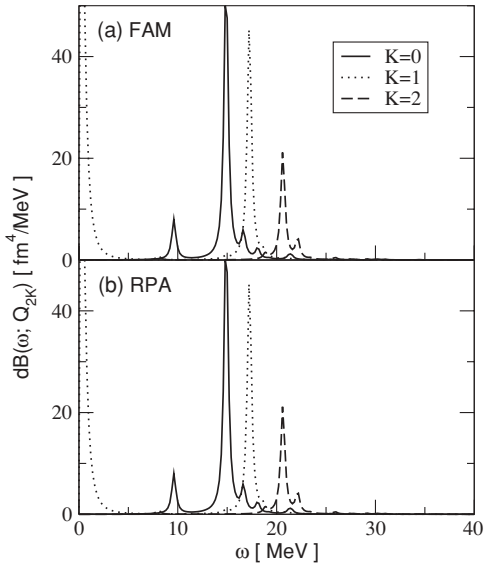

FIG. 1. IS quadrupole strength distribution for ^{20}Ne, with $K = 0$, 1, and 2. Results are compared from two kinds of calculations: (a) the finite amplitude method (FAM) and (b) the conventional RPA.

because the nucleus actually rotates in real time, which violates the small-amplitude approximation. This is an advantage of the present method over the time-dependent approach. The lowest intrinsic (physical) excitation corresponds to the $K = 2$ mode at $\omega = 8$ MeV, which is close to the energy of the 1p1h excitation. This suggests that the correlation effect is weak for this mode, supported by a small $K = 2$ quadrupole strength at $\omega = 8$ MeV. In contrast, the next lowest mode at $E_x = 9.6$ MeV with $K = 0$ is somewhat lowered by the correlation and exhibits a larger strength. Reference [18] shows the results of the configuration mixing calculation with the BKN interaction, indicating $J^\pi = 0^+$ around $E_x = 7$ MeV and $J^\pi = 2^+$ state near 8 MeV. Large peaks at $\omega = 15 \sim 22$ MeV should correspond to the IS giant quadrupole resonance. It clearly shows deformation splitting: the $K = 0$ peak at the lowest, the $K = 1$ in the middle, and the $K = 2$ at the highest energy.

Now, let us demonstrate the accuracy of the present finite amplitude method. In Fig. 1, results of the conventional RPA, which explicitly estimates the residual interactions $\delta h/\delta\rho$, are presented in panel (b). These two kinds of calculations, FAM and RPA, provide identical results in the accuracy of three to four digits.

2. Isoscalar dipole and octupole responses: Removal of NG modes

Next, we show the strength distribution for the isoscalar compressional dipole mode. This mode has been of significant interest because its energy is related to the compressibility of nuclear matter, providing information independent from the monopole resonance. The compressional modes in spherical nuclei have been extensively studied with the continuum RPA calculations [19–21]. However, these calculations are not fully self-consistent; thus, there is the need to remove a

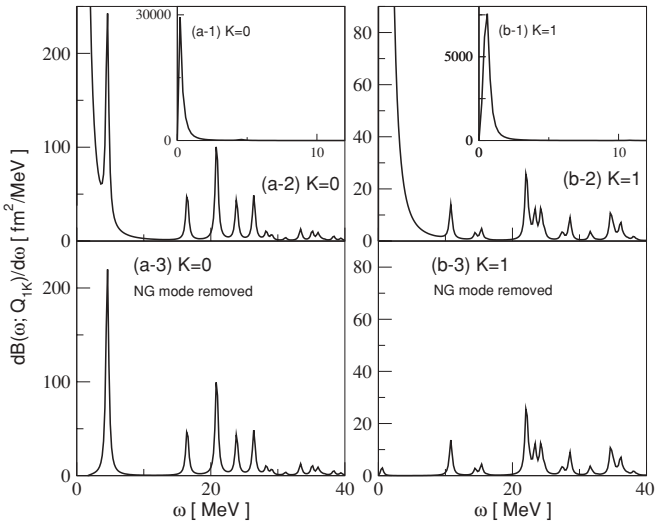

FIG. 2. IS compressional dipole strength distribution for ^{20}Ne. Strengths associated with the $K = 0$ modes are shown in the left (a) and those with $K = 1$ in the right (b). The upper panels show strengths calculated with $\delta\rho_{\rm cal}(\omega)$, while the lower panels, (a-3) and (b-3), show those calculated with $\delta\rho_{\rm phy}(\omega)$ in Eq. (44). See text for details.

mixture of the NG (translational) components by modifying the dipole operator. This produces some ambiguity in their results. In fact, the importance of the full self-consistency has been stressed for the compressional modes [22,23]. So far, our understanding of the compressional dipole mode is still obscure, and further studies are needed. In this section, we show a fully self-consistent calculation for deformed nuclei.

In Fig. 2, the compressional dipole strength is shown for the $K = 0$ mode at the left (a) and the $K = 1$ mode at the right (b). The NG modes associated with the translational symmetry breaking near $\omega = 0$ are seen in Fig. 2, insets (a-1) and (b-1). These NG peaks are so huge that other peaks are invisible in these insets. The vertical axis is magnified in panels (a-2) and (b-2). The giant resonance peaks are spread over $\omega = 16 \sim 30$ MeV for $K = 0$ and 20–40 MeV for $K = 1$. There is a sharp peak at $\omega = 4.5$ MeV, which is embedded in the tail of the NG mode. To estimate the strength carried by this state, we need to separate out the contribution from the NG mode. This is done by using the prescription described in Sec. II D, adopting the center-of-mass coordinates and the total linear momenta (three NG modes). Strength associated with the physical transition density $\delta\rho_{\rm phy}(\omega)$ is shown in Figs. 2(a-3) and 2(b-3). The large strength of the translational modes is properly removed. The other physical peaks with finite ω are unchanged, which indicates that there is very little mixture of the NG modes because our calculation is fully self-consistent. Now, we may identify the $K = 0$ peak at $\omega = 4.5$ MeV as an isolated peak.

Finally, we show IS octupole strength distributions with $K = 0$, 1, 2, and 3 in Fig. 3. The lowest octupole state is at $\omega = 4.5$ MeV with $K = 0$, and the second lowest is at $\omega = 8.1$ MeV with $K = 2$. These results are similar to those of the variation-after-parity-projection calculation [24] and the configuration-mixing calculation [18]. Experimentally, the bandhead of the $K = 2$ band ($J^\pi = 2^-$) is observed at $E_x = 5.0$ MeV and that of $K = 0$ ($J^\pi = 1^-$) is at $E_x = 5.8$ MeV. The BKN interaction, which does not contain the spin-orbit force, is able to reproduce the $K = 0$ state in a reasonable accuracy; however, it fails to provide a quantitative description for the $K = 2$ state. This suggests that the spin-orbit force does not play an important role for the $K = 0$ state. In fact, the parity-projected HF calculation with the Skyrme interaction has confirmed very small contribution of the spin-orbit force in this $K^\pi = 0^-$ state [25].

Since the nucleus is deformed, the dipole modes are coupled to the octupole modes. We can identify peaks at the same positions in Figs. 2 and 3 for the $K = 0$ and $K = 1$. We see a small spurious $K = 1$ peak near $\omega = 0$, even after removing the NG components [solid line in Fig. 3(b)]. However, the peak height of the NG mode is about 5000 fm^6/MeV. Thus, more

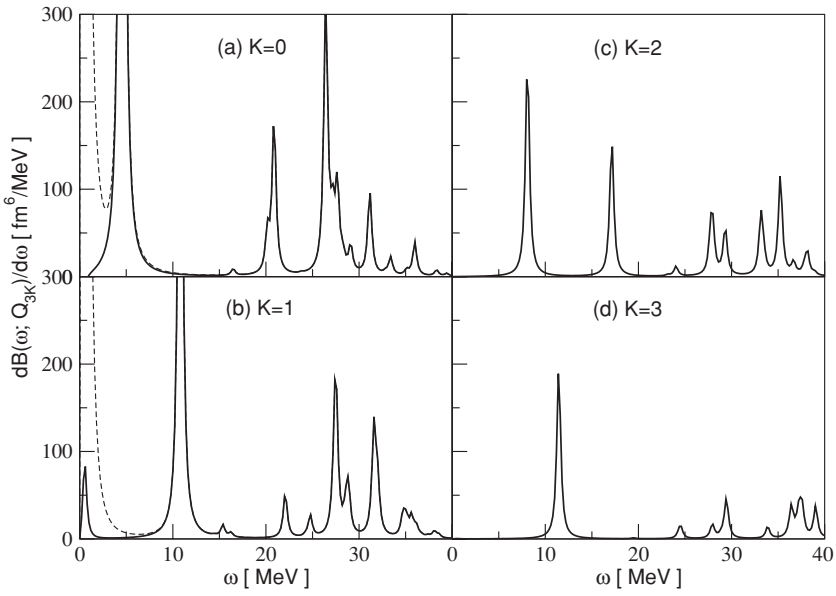

FIG. 3. IS octupole strength distribution for ^{20}Ne associated with the $K = 0$, 1, 2, and 3 octupole modes. In panels (a) and (b), the strengths calculated with $\delta\rho_{\rm cal}(\omega)$ are presented by dotted lines, those with $\delta\rho_{\rm phy}(\omega)$ by solid lines.

than 98% of the NG strength is actually removed. We can say that the method in Sec. II D also works for octupole modes.

IV. CONCLUSION AND DISCUSSION

We have presented a new numerical approach to the RPA calculation: the finite amplitude method. The finite amplitude method does not require complicated programming for complex residual interactions. Instead, it resorts to the numerical derivation of the residual interaction (induced field), $\delta h/\delta\rho \cdot \delta\rho$. The most advantageous feature of this method is its feasibility in programming a computer code. The RPA calculation can be accomplished with a minor extension of the static HF computer code, to construct the HF Hamiltonian with independent bra and ket single-particle states.

Here, we would like to remark on the meaning of different bra and ket states. This does not mean matrix elements between different Slater determinants, which are rather complicated. These "off-diagonal" elements are necessary for configuration-mixing calculations, such as the generator-coordinate method. The finite amplitude method does not require these. All we need is "diagonal" matrix elements of a certain one-body operator, $\hat{o}$, in the linear order with respect to the variation of the single-particle states, that is,

$$\sum_{i=1}^{A}\langle\psi_i|\hat{o}|\psi_i\rangle \approx \sum_{i=1}^{A}\langle\phi_i|\hat{o}|\phi_i\rangle + \sum_{i=1}^{A}\langle\delta\psi_i|\hat{o}|\phi_i\rangle + \sum_{i=1}^{A}\langle\phi_i|\hat{o}|\delta\psi_i\rangle. \quad (61)$$

To separately calculate the second and the third terms in the right-hand side, we need to input independent bra and ket single-particle states. This can be achieved by a minor extension of the static HF code.

The method has been applied to calculations of the isoscalar dipole, quadrupole, and octupole response functions. Since the adopted interaction is rather schematic, we do not discuss here the calculated properties of these modes. Instead, we would like to emphasize the characteristic features of the finite amplitude method. First of all, the transition density coupled to the NG modes can be calculated without any special treatment. This is an advantage over the real-time small-amplitude TDHF [11]. Second, since we do not calculate the residual interaction explicitly, it is easy to carry out the fully self-consistent RPA calculation for realistic interactions including spin-orbit, derivative, and Coulomb terms. The implementation of the present method does not depend on the complexity of the interactions. For instance, the compressional dipole mode has been a long-standing problem in microscopic calculations [26]. The problem is related to difficulties in the fully self-consistent treatment and in the coupling to the translational modes. Very recently, effects of the self-consistency violation have been investigated in detail for spherical nuclei [27]. Our new approach may provide a practical tool for investigating deformed nuclei. Last but not least, the finite amplitude method is an efficient method for calculating the strength distribution. We may control the necessary energy resolution by the smoothing parameter Γ. The numerical application to the BKN functional shows that its efficiency is next to the time-dependent method, better than other methods including the Green's function method [11] and the diagonalization method [16]. The diagonalization of the RPA matrix is very efficient if we are interested in only a few lowest states; however, it becomes more and more difficult for higher excitation energies.

For future developments, it is interesting to combine the present method with the absorbing-boundary-condition approach in Ref. [11]. This enables us to calculate response in the continuum, overcoming difficulties in the time-dependent method. It is also very interesting to extend the method in the HF scheme to the one in the Hartree-Fock-Bogoliubov framework. In this paper, we adopt a simple interaction to check the method, but the finite amplitude method shows its real power for a complex density functional. Applications of the method to the realistic Skyrme functionals are under progress at present and will be published in near future.

ACKNOWLEDGMENTS

This work is supported by the Grant-in-Aid for Scientific Research in Japan (Nos. 17540231, 18540366, 18036002), by the PACS-CS project of the Center for Computational Sciences, University of Tsukuba, and by the Large Scale Simulation Program No. 06-14 (FY2006) of the High Energy Accelerator Research Organization (KEK). Part of the numerical calculations were performed on the supercomputer at the Research Center for Nuclear Study (RCNP), Osaka University, and at YITP, Kyoto University.

[1] M. Bender, P. H. Heenen, and P.-G. Reinhard, Rev. Mod. Phys. **75**, 121 (2003).
[2] D. Lunney, J. M. Pearson, and C. Thibault, Rev. Mod. Phys. **75**, 1021 (2003).
[3] P. Ring and P. Schuck, *The Nuclear Many-Body Problems* (Springer-Verlag, New York, 1980).
[4] J. Terasaki, J. Engel, M. Bender, J. Dobaczewski, W. Nazarewicz, and M. Stoitsov, Phys. Rev. C **71**, 034310 (2005).
[5] G. Giambrone, S. Scheit, F. Barranco, P. F. Bortignon, G. Colò, D. Sarchi, and E. Vigezzi, Nucl. Phys. **A726**, 3 (2003).
[6] D. Vretenar, N. Paar, P. Ring, and G. A. Lalazissis, Nucl. Phys. **A692**, 496 (2001).
[7] N. Paar, P. Ring, T. Nikšić, and D. Vretenar, Phys. Rev. C **67**, 034312 (2003).
[8] T. Nakatsukasa and K. Yabana, Prog. Theor. Phys. Suppl. **146**, 447 (2002).
[9] H. Imagawa and Y. Hashimoto, Phys. Rev. C **67**, 037302 (2003).
[10] T. Inakura, M. Yamagami, K. Matsuyanagi, S. Mizutori, H. Imagawa, and Y. Hashimoto, Int. J. Mod. Phys. E **13**, 157 (2004).
[11] T. Nakatsukasa and K. Yabana, Phys. Rev. C **71**, 024301 (2005).
[12] A. S. Umar and V. E. Oberacker, Phys. Rev. C **71**, 034314 (2005).

[13] P. Bonche, S. Koonin, and J. W. Negele, Phys. Rev. C **13**, 1226 (1976).
[14] J.-P. Blaizot and G. Ripka, *Quantum Theory of Finite Systems* (MIT, Cambridge, MA, 1986).
[15] G. Bertsch and S. F. Tsai, Phys. Rep. **18**, 125 (1975).
[16] A. Muta, J.-I. Iwata, Y. Hashimoto, and K. Yabana, Prog. Theor. Phys. **108**, 1065 (2002).
[17] H. Flocard, S. E. Koonin, and M. S. Weiss, Phys. Rev. C **17**, 1682 (1978).
[18] S. Shinohara, H. Ohta, T. Nakatsukasa, and K. Yabana, Phys. Rev. C **74**, 054315 (2006).
[19] N. van Giai and H. Sagawa, Nucl. Phys. **A371**, 1 (1981).
[20] I. Hamamoto, H. Sagawa, and X. Z. Zhang, Phys. Rev. C **57**, R1064 (1998).
[21] S. Shlomo and A. I. Sanzhur, Phys. Rev. C **65**, 044310 (2002).
[22] B. K. Agrawal, S. Shlomo, and A. I. Sanzhur, Phys. Rev. C **67**, 034314 (2003).
[23] B. K. Agrawal and S. Shlomo, Phys. Rev. C **70**, 014308 (2004).
[24] S. Takami, K. Yabana, and K. Ikeda, Prog. Theor. Phys. **96**, 407 (1996).
[25] H. Ohta, K. Yabana, and T. Nakatsukasa, Phys. Rev. C **70**, 014301 (2004).
[26] N. van Giai, P. F. Bortignon, G. Colo, Z. Ma, and M. Quaglia, Nucl. Phys. **A687**, 44c (2001).
[27] T. Sil, S. Shlomo, B. K. Agrawal, and P.-G. Reinhard, Phys. Rev. C **73**, 034316 (2006).